Summer School "Governing Climate Engineering", 12 – 16 July 2010, Heidelberg, Germany

Climate response to major volcanic eruptions in earth system climate models of different complexities

Doreen Metzner (1), M. Toohey (1), S. Lorenz (2), U. Niemeier (2), V. Brovkin (2), S. Kutterolf (1), A. Freundt (1), C. Timmreck (2), K. Krüger (1)
(1) IFM-GEOMAR, Kiel, Germany; (2) Max-Planck-Institute for Meteorology, Hamburg, Germany

Motivation

One of the most important natural causes of climate change are major volcanic eruptions as they have an significant impact on the Earth's global climate system (Fig. 1). To evaluate the climate response to major volcanic eruptions we use the Earth System Model of Intermediate Complexity (EMIC) CLIMBER by forcing it with a new radiative forcing data set comprising large Plinian eruptions from volcanoes at the Central American Volcanic Arc (CAVA) over the last 200 ka. This specifically created radiative forcing data set is based on the "petrological method" and use information about strength and height of the volcanic sulphur injection *(1, 2)*. Our first evaluation involves simulations forced with the assessed radiative forcing of the largest CAVA eruption (~700 Mt SO_2) Los Chocoyos (84 ka). By comparing these runs with simulations of the best observed large volcanic eruption, the one of Mt Pinatubo in June 1991 (~17 Mt SO_2), we analyse similarities and differences, which may be generated by complex relationships between the radiative forcing and the climate system. The same set of forcing is also used for simulations with the complex Earth System Model (ESM) from MPI. Similarities and differences between the two different model runs will be used for a better understanding of the complex climate interactions after major volcanic eruptions. We consider global atmospheric effects, as soon as possible changes in the ocean circulation, the carbon cycle and vegetation will follow.

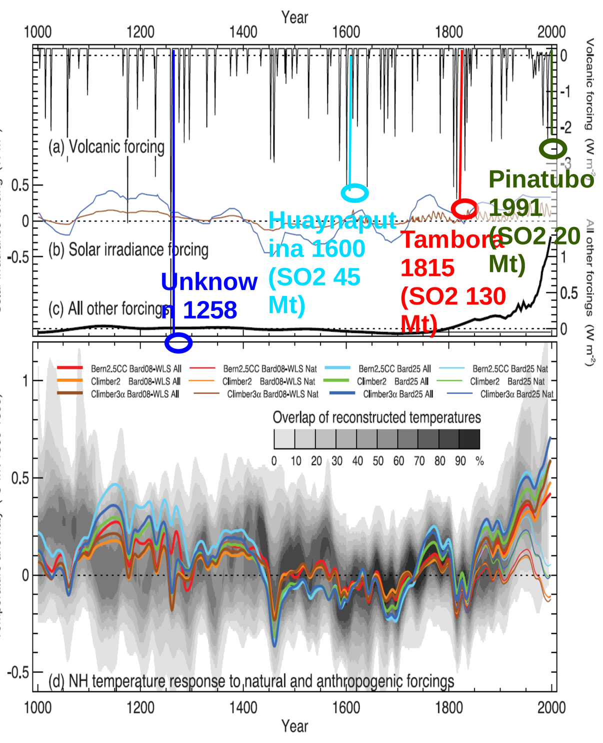

Fig. 1: Radiative forcings (a-c) and simulated annual NH temperatures (°C) during the last 1.1 kyr simulated by 3 climate models under the forcings (d), compared with the concentration of overlapping NH temperature reconstructions (shown by grey shading). 'All' (thick lines) used anthropogenic and natural forcings; 'Nat' (thin lines) used only natural forcings (IPCC, 2007).

Earth System Climate Models (ESM)

CLIMBER

Fast Earth System Climate Model of Intermediate Complexity (EMIC)
CLIMBER-2: CLIMate and BiosphERe *(3)*

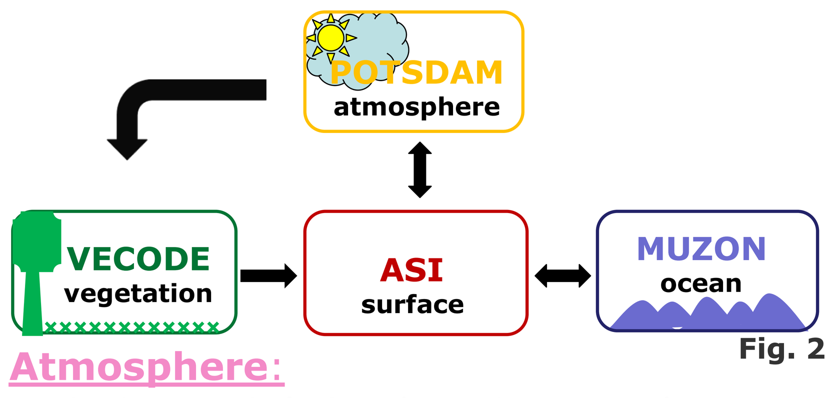

Fig. 2

Atmosphere:
- POTSDAM-2 (POTsdam-Statistical-Dynamical Atmosphere Model *(4, 3)*), 2.5 dimensional **dynamical-statistical atmosphere model**

Ocean:
- MUZON (MUltibasin ZONally Averaged Ocean Model *(5)*), **zonally averaged**, 3 basins (incl. sea ice), no El Niño-Southern Oscillation (ENSO) is resolved

Land/Vegetation:
- VECODE (VEgetation COntinuous DEscription Model *(6, 7)*), **dynamical global** vegetation model, including terrestrial carbon pools

MPI-M ESM

Complex Earth System Model
MPI-M ESM: Max-Planck-Institute for Meteorology Earth System Model *(8)*

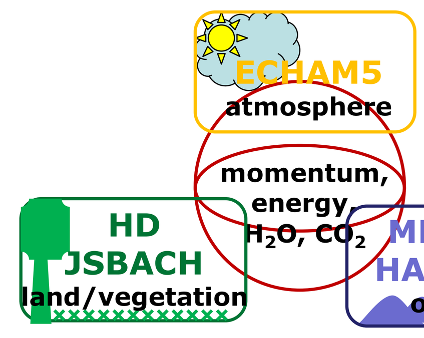

Fig. 3

Atmosphere:
- ECHAM5 (European Center/ HAMburg model, *(9)*), T31/L19, **GCM**

Ocean:
- MPIOM (Max-Planck-Institute Ocean Model *(10)*), 3°L40, **ocean and sea ice**, high variability due to ENSO
- HAMOCC5 (HAMburg Ocean Carbon Cycle *(11, 12)*), 3-dimensional

Land/Vegetation:
- JSBACH (Jena Scheme for Biosphere-Atmosphere Coupling in Hamburg *(13)*)
- HD (Hydrological Discharge model *(13, 14)*)

Los Chocoyos vs. Pinatubo eruption

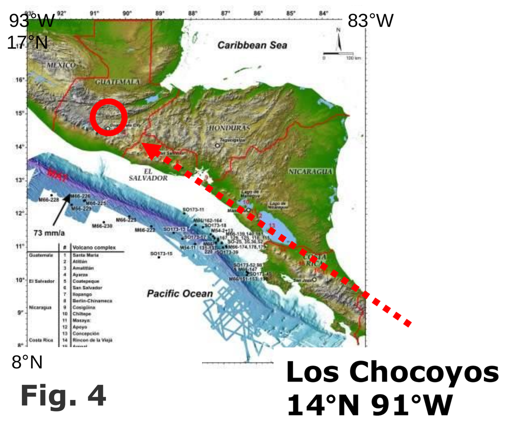

Fig. 4

Los Chocoyos (LC):
- VEI (Volcanic Explosivity Index) 7
- Last eruption: 84 ka BP
- **670 Mt SO_2**
- Measured by petrological method
- Largest eruption of ~30 major volcanic eruptions of the (CAVA) time series of the last 200 ka *(1, 2)*

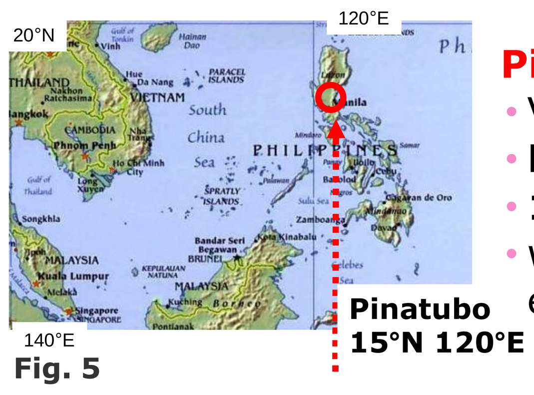

Fig. 5

Pinatubo (PI):
- VEI 5
- Last eruption: 1991
- **17 Mt SO_2**
- well detected and investigated eruption

Compilation of the volcanic forcing

Based on the atmospheric SO_2 injection (minimum value) and using simple linear relationship, we derive (Tab. 1):
- **Stratospheric aerosol optical depth** (AOD) (τ_D): simple linear relationship *(16, 17)*, power of 2/3 relation for eruptions >10 Mt SO_2 **(a)**
- **Radiative forcing** calculation after *(18)* ($\Delta f_{net}=\sim 23.5\tau$ [W/m²]) **(b)**

Unit	Acro-nym	Age [ka]	SO_2 [Mt] (min)	(a) Max. Stratospheric Optical Depth (τ_D)	(b) Radiative forcing $\Delta f_{net}=(\sim 23.5\tau)$ [W/m²] (Lacis et al., 1992)
Pinatubo (1991) (PHI)	PI	0.02	**17**	0.180	**-4.22**
Los Chocoyos (GUA)	LC	84	**668.62**	2.380	**-55.81**

Tab. 1

Validation of the SO_2–AOD relationship

Simulations of a number of CAVA eruptions of different magnitudes with the model MAECHAM5 (T42/L39) with the HAM aerosol microphysics module *(19)* (Fig. 6)

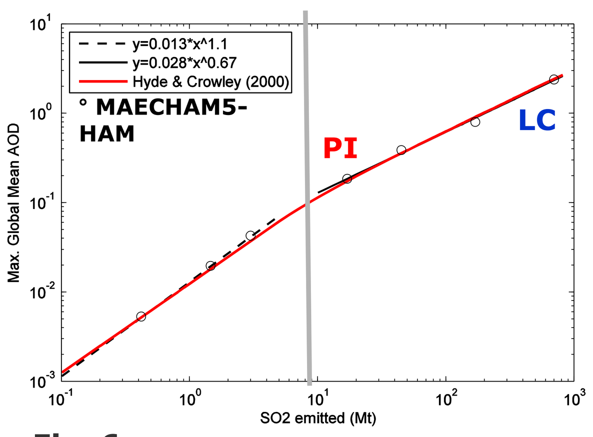

Fig. 6 (M. Toohey)

- **Change of slope** between the smaller eruptions (<10 Mt SO_2) and the larger ones
- Fits showing the relationship was **nearly linear for smaller eruptions** and a **function of the SO_2 emitted to the power of 2/3 for larger ones**
- **Transition point around 10 Mt SO_2** (*(20)* used 15 Mt SO_2 , consistent with *(21)*)

Results

Simulations of LC and PI

CLIMBER:
- Forces with reduced solar constant by **annual global mean radiative forcing**

Monthly radiative forcing for LC and PI

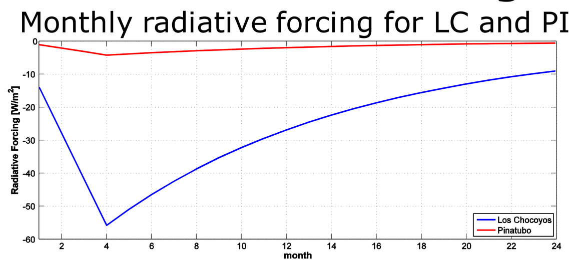

Fig. 7

MPI-M ESM:
- Forced with **monthly AOD** simulated with MAECHAM5-HAM
- **Latitude resolved** AOD forcing

Monthly AOD forcing for LC

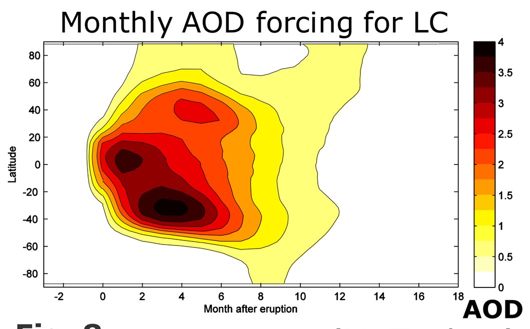

Fig. 8 (M. Toohey)

Monthly Surface Air Temperature (SAT) anomalies

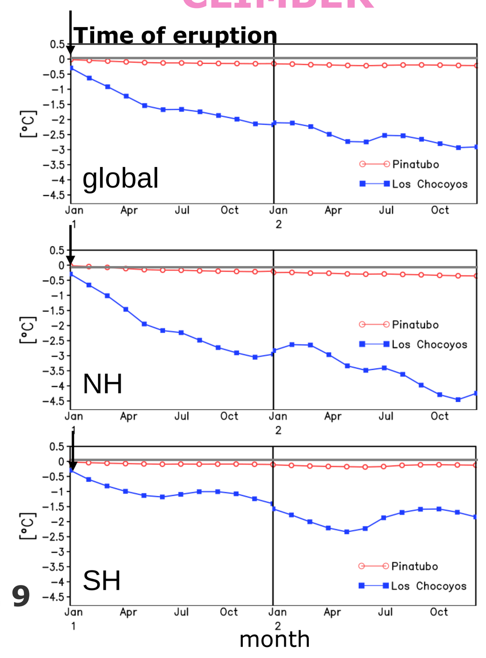

Fig. 9

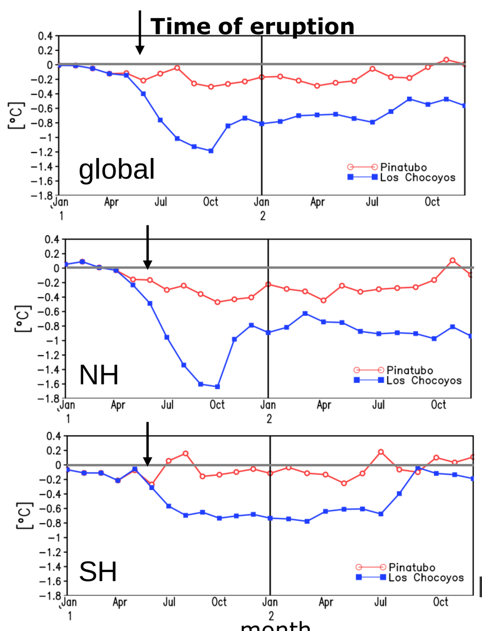

Fig. 10

- SAT decreases after PI and LC, respectively, in particular for the CLIMBER simulations (Fig. 9, 10) and for Northern Hemisphere (NH) due to high land fraction
- The SAT anomalies for PI are in both models similar, whereas for LC the differences are clearly seen
- The variability is large in the MPI-M ESM runs (Fig. 10) in comparison to the almost non variability in CLIMBER (Fig. 9)

Seasonal SAT and Precipitation (PRC) anomalies

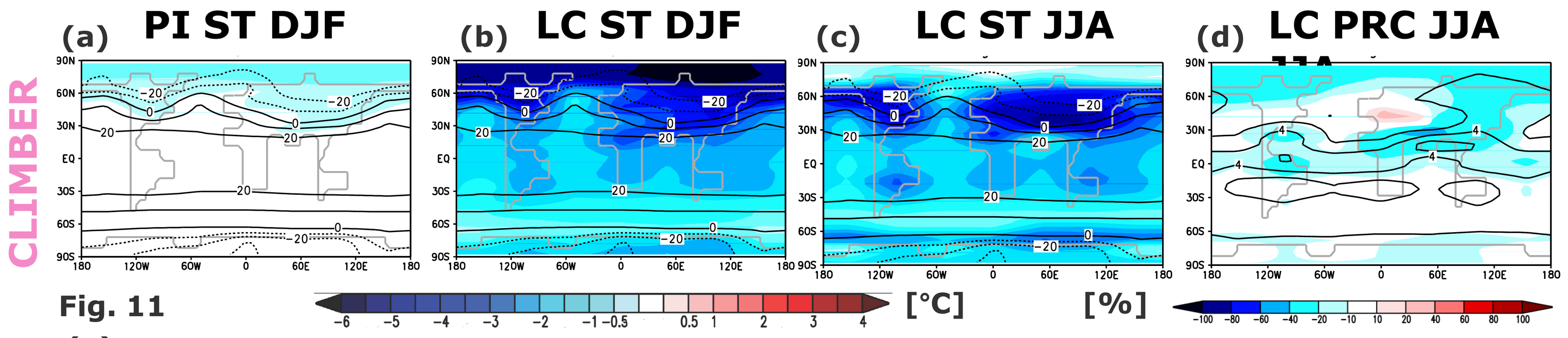

Fig. 11

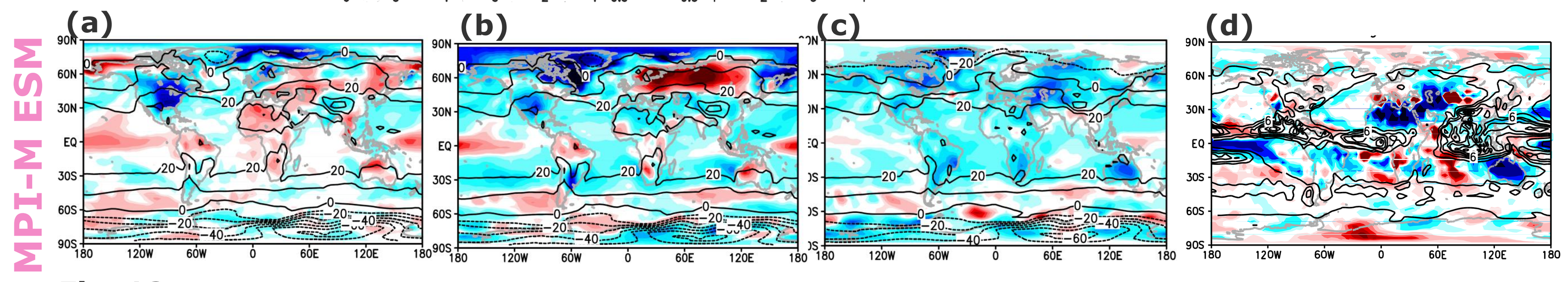

Fig. 12

- Shown is the mean of the two winter s(DJF) and summers (JJA), respectively
- The observed warming in the NH winter season and the cooling in the summer season after the eruption is in particular seen in the MPI-M ESM (Fig. 12a-c).
- Overall cooling, especially over (NH) continents, is seen in CLIMBER (Fig. 11a-c)
- Reduced summer precipitation is seen in the tropics (Fig. 11d, 12d), with a larger global averaged reduction of -12% for CLIMBER than -5% for MPI-M ESM
- Whereas in Climber the anomalies for LC are one magnitude larger than for PI the differences between the two eruptions are not so large in the MPI-M ESM
- Global averaged magnitude of the anomalies for PI are similar in both models (~-0.2°C), however the differences for LC between the two is high (CLIMBER: ~-2.3°C, MPI-M ESM: ~-0.7°C)
– causes?: different variability, radiative forcing)

Yearly SAT and SeaIce Extent (SIE) anomalies (only for CLIMBER)

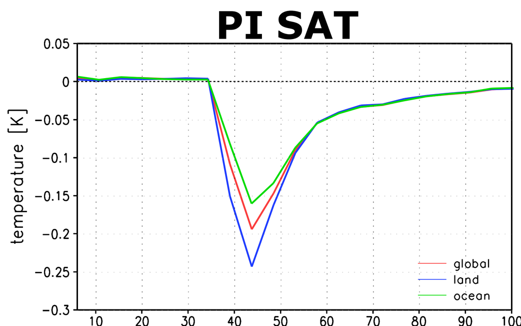

Fig. 13

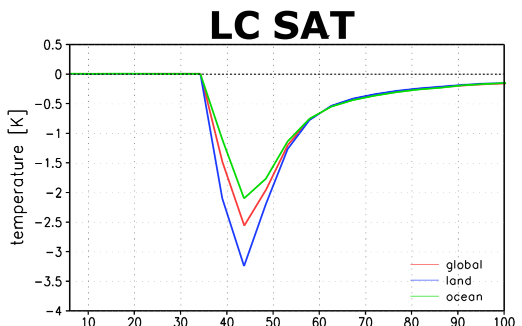

Fig. 14

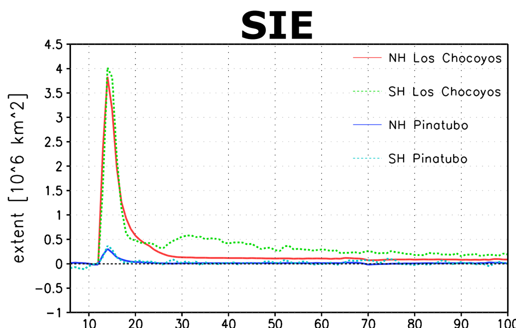

Fig. 15

- The annual mean SAT anomalies are larger over the land as over the ocean, as expected (Fig. 13, 14)
- There is a clear signal for both hemispheres in the sea ice extent increasing after the LC eruption more than for the PI eruption (nearly one magnitude) (Fig. 15)

Outlook

- Analysis further effects/feedbacks, e.g. ocean (heat content, MOC) and vegetation response
- Revising the MPI-M ESM forcing and performance of more MPI-M ESM simulations
- Climber simulations for different time periods of the whole CAVA time series (Glacial/Interglacial mode)

References

1) Kutterolf et al., The Pacific offshore record of Plinian arc volcanism in Central America: 1. Along-arc correlations, Geochem. Geophys. Geosystems, 9, 2008a.
2) Kutterolf et al., The Pacific offshore record of Plinian arc volcanism in Central America: 2. Tephra volumes and erupted masses, Geochem. Geophys. Geosystems, 9, 2008b
3) Petoukhov et al., CLIMBER2: A climate system model of intermediate complexitiy. Part I: model description and performance for present climate, Clim. Dyn., 16, 1-17, 2000.
4) Petoukhov, V. and Ganopolski, A set of climate models for integrated modelling of climate change impacts. Part II: A 2.5-dimensional dynamical-statistical climate model (2.5-DSCM), IIASA WP-94-39, 96pp, 1994.
5) Stocker et al., A zonally averaged coupled ocean-atmosphere model for paleo climate studies, J. Clim., 5, 773-797, 1992.
6) Cramer et al., Global response of terrestrial ecosytem structure and function to CO2 and climate change: results from six dynamic global vegetation models, Global Change Biology, 7, 357-373, 2001.
7) Brovkin et al., Carbon cycle, Vegetation and Climate Dynamics in the Holocen: Eperiments with the CLIMBER-2 Model, Global Biogechem., Cycles, 16, 1139,20pp, 2002.
8) Jungclaus et al., Climate and carbon-cycle variabililty over the last Millenium, Clim Past, submitted.
9) Roeckner et al., 2003, The atmospheric general circulation model ECHAM5. Part I Model description, Tech. Rep. 349, 127pp, MPI for Meteorology HH, 2003.
10) Marsland et al., The Max Planck Institute global ocean/sea ice model with orthogonal curvilinear coordinates, Ocean Modell., 5, 1191-127, 2003.
11) Maier-Reimer et al., The HAMburg Ocean Carbon Cycle Model HAMOCC5.1 – Technical description releas 1.1. Rep. 14. MPI for Meteorolgoy HH, 57pp. 2005.
12) Wetzel et al., 2006, Effects of Ocean Biology on the Penetrative Radiation in a Coupled Climate Model, J. Clim., 19, 3973-3987, 2006.
13) Raddatz et al., Will the tropical land biosphere dominate the climate-carbon feeback during the twenty-first century? Clim. Dynam., 29, 565-574, 2007.
14) Hagemann, S. and L. Dümenil, A parameterization of the lateral waterflow for the global scale, Clim. Dynam., 14, 17-31, 1998.
15) Hagemann, S. and L. Dümenil, Validation of the hydrological cycle of ECMWF and NCEP reanalyses using the MPI hydrological discharge model., J. Geophys. Res., 106, 1503-1510, 2001.
16) Stothers, R. B., The great Tambora eruption in 1815 and its aftermath, Science, 224, 1191-1198, 1984a.
17) Stothers, R. B., Mystery cloud of AD 536, Nature, 307, 344-345, 1984b.
18) Lacis et al. , Climate forcing by stratospheric aerosols, Geophys. Research Letter, 19, 1607-1610, 1992.
19) Niemeier et al., Initial fate of fine ash and sulfur from large volcanic eruptions, ACP, 9, 9043-9057, 2009.
20) Crowley, T., Causes of climate change over the past 1000 years, Science, 289, 270-277, 2000.
21) Hyde, W. and T. Crowley, Probability of future climatically significant volcanic eruptions, J. Clim., 13, 1445-1450, 2000.

contact: dmetzner@ifm-geomar.de